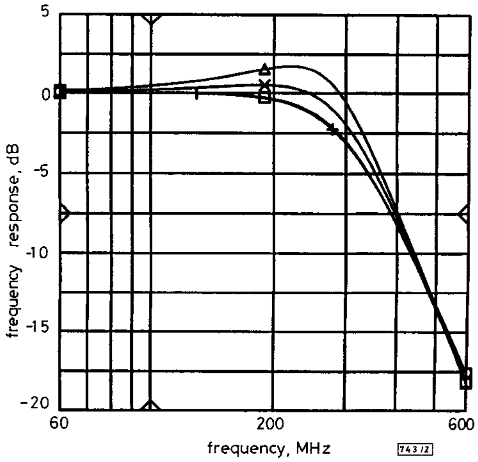

Fig. 2 *Lowpass filter frequency responses*

△ equal valued capacitor design
× unity gain amplifier design
□ ideal response
+ simulated response of HBT design

C_3, in the filter, was reduced to account for the parasitic input capacitance of the emitter follower. Note that the frequency response of this filter is nearly identical to an ideal third order response and that this filter has a corner frequency of 300MHz, which is significantly higher than can be achieved with typical active filters. Thus, this design demonstrates the practicality of using unity gain amplifiers to create high performance active filters.

27 March 1995
Electronics Letters Online No: 19950601

B.A. Kramer (*Rockwell International, 400 Collins Road NE, Cedar Rapids, IA 52498, USA*)

References

1 AIKENS, R.S., and KERWIN, W.J.: 'Single amplifier, minimal RC, Butterworth, Thomson, and Chebyshev filters to sixth order'. Proc. Int. Filter Symp., Santa Monica, CA, 1972, pp. 81–82

2 HUELSMAN, L.P.: 'Equal-valued-capacitor active-RC-network realisation of a 3rd-order lowpass Butterworth characteristic', *Electron. Lett.*, 1971, **7**, pp. 271–272

Adaptive fixed-length differential chain coding for transmission of line graphics

H. Yuen and L. Hanzo

Indexing terms: Computer graphics, Image processing

An adaptive fixed-length differential chain coding (FL-DCC) scheme is introduced for transmission of line graphics. Compared to differential chain coding (DCC), which uses vectors with different lengths, FL-DCC has a lower coding rate and a more uniform data syntax while maintaining a comparable subjective graphical quality.

Introduction: Telewriting is a multimedia telecommunication service enabling bandwidth-efficient transmission of encoded handwritten text and line graphics through communication networks where a low bit rate is important. On the other hand, the codes should be designed such that the decoding process would not be corrupted by transmission errors therefore enabling data synchronisation to be maintained, particularly in mobile communications environments where the channel quality is typically poor. Differential chain coding (DCC) was developed for dynamographical communications over telephone or e-mail networks connecting personal computers with EGA (640 × 350 pixels) resolution [1], where bit rate economy is achieved by exploiting the correlation between successive vectors. However, since DCC uses vectors with different bit lengths, a 2 bit prefix for absolute vectors is necessary to distinguish them from the three 2 bit relative vectors [2, 3]. Apparently, DCC is in, general, less efficient than chain difference coding and the prefix is vulnerable to transmission errors. The decoding process is easily corrupted due to either errors in the prefix or errors in the relative vector, which cause it to become the pattern of the prefix [2]. To overcome these problems, an adaptive fixed-length differential chain coding scheme (FL-DCC) is introduced in this Letter. A fixed length of bits is used to encode a smaller differential vector set which is adaptively defined from the vector differences. In this way FL-DCC offers a lower coding rate and a more uniform data syntax than DCC while still maintaining a comparable subjective quality.

Fixed-length differential chain coding (FL-DCC): A square coding ring is slid in steps along the successive points of a trace from the line graphics. The coding ring has sides of $2n\tau$ and contains $M = 8n$ nodes, where $n = 1, 2, 3, \ldots$ is the order of the ring and τ is the spacing of the ring. The first vector displacement along the trace is the best fitting vector defined by standard chain coding (SCC). The coding ring is then translated along this starting vector to determine the next vector along the trace. A differential approach is employed for the encoding of all the following vectors along the trace, in which the difference in direction between the present vector and its previous vector is calculated, and all possible $8n$ vector differences are mapped into a 2^b differential vector set consisting of b bit fixed-length codewords, where $8n \geq 2^b$. Fig. 1 illustrates the coding principles of FL-DCC for $b = 2$ and $M = 8$. Some of the low probability vector differences have been combined with the neighbouring vector differences, making the differential vector set smaller than the vector differences. Therefore, FL-DCC is a lossy differential chain coding scheme. It is based on the statistical properties of handwriting and drawings that the probability of large vector differences is generally small [1]. The differential vector set of FL-DCC is designed such that the quantisation distortion is minimised and it is adaptive to the statistical nature of the line graphics.

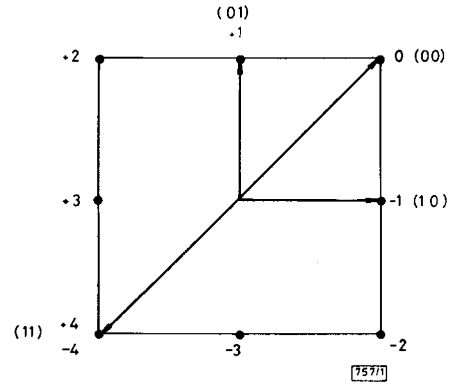

Fig. 1 *Principles of FL-DCC for $b = 2$, $M = 8$*

vector difference	coded as (b = 2)	decoded as
0	00	0
+1, +2	01	+1
−1, +2	10	−1
+3, ±4, −3	11	±4

The data syntax of the FL-DCC scheme is shown in Fig. 2, where a trace starts with a pen-down (PD), followed by a number of vectors and ends with a pen-up (PU). The starting co-ordinates X_0 and Y_0 of the trace are directly encoded using 10 and 9 bits, respectively, for a VGA resolution of 640 × 480 pixels. The starting vector (SV) is encoded by SCC using $I[\log_2 8n]$ bits, where $I[x]$ denotes the smallest integer greater than or equal to x. All vectors afterwards are b bit fixed-length, which results in a simple and more uniform data syntax than DCC.

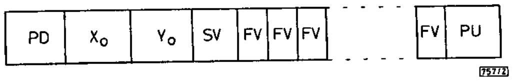

Fig. 2 *Data syntax of FL-DCC*

PD: pen-down	(1 byte)
X_0: X-co-ordinate of trace origin	(10 bits)
Y_0: Y-co-ordinate of trace origin	(9 bits)
SV: starting vector	($J\lceil\log_2 8n\rceil$ bits
FV: fixed-length vector	(b bits)
PU: pen-up	(1 byte)

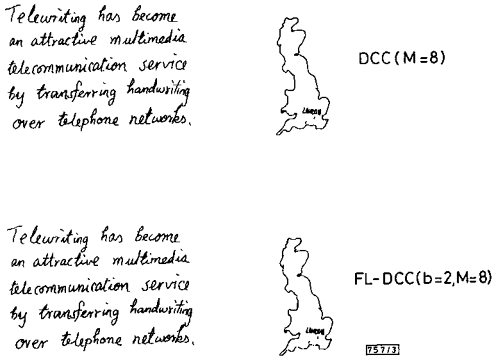

Fig. 3 *Decoded source signals for DCC (M = 8) and FL-DCC (b = 2, M = 8)*

Coding rate: The coding rate of a chain code is defined as the number of bits produced by the code per unit length of the curve segment. A low coding rate corresponds to a higher coding efficiency [4]. When a curve is encoded by FL-DCC, it is sliced by the coding ring into small segments. Consider a sampled curve segment s. Let v be the corresponding vector link produced by the coding ring of order n. The coding rate of FL-DCC is given by

$$r = \frac{E[b(s,v)]}{E[l_n(s)]} \qquad (1)$$

where $b(s, v)$ is the number of bits used to encode the vector link v, and $l_n(s)$ is the length of curve segment s for a coding ring of order n. $E[x]$ represents the expected value of a random variable x. Using the assumption that the product of a segment length, and the probability $p(\alpha)$ that this segment occurs with a direction α remains constant, the expected length of the curve segment s becomes

$$E[l_n(s)] = 8\int_0^{\pi/4} \frac{n\tau}{\cos\alpha} p(\alpha)d\alpha = \frac{\pi n \tau}{2\sqrt{2}} \qquad (2)$$

Using eqns. 1 and 2, the theoretical coding rate of FL-DCC is

$$r = \frac{2\sqrt{2}E[b(s,v)]}{\pi n \tau} \qquad (3)$$

Table 1: Coding rate comparison for FL-DCC (b = 2), DCC and SCC with coding ring of M = 8, τ = 1

	Coding rate (bits per unit length)		
	FL-DCC	DCC	SCC
English script	1.73	2.02	2.71
Chinese script	1.75	2.04	2.66
Map	1.74	2.04	2.71
Drawing	1.79	1.94	2.74
Theoretical coding rate	1.80	2.03	2.70

Experimental results: The performance of the FL-DCC scheme was evaluated for a range of dynamographical source signals including an English script, a Chinese script, a drawing and a map with a coding ring of M = 8. Table 1 shows the associated coding rates produced by FL-DCC (b = 2), DCC and SCC along with the corresponding theoretical coding rates. It can be seen that FL-DCC achieves a lower coding rate than DCC and SCC, from both the theoretical results and the experimental measurements. The corresponding subjective quality is portrayed in Fig. 3 for two of the source signals. No subjective degradation is observed for FL-DCC (b = 2) when compared to DCC.

Conclusions: By employing an adaptively defined differential vector set that is smaller than the vector differences, FL-DCC offers higher coding efficiency than DCC and SCC while maintaining comparable subjective quality. The fixed-length codes of FL-DCC would not cause decoding confusion between vectors in the presence of transmission errors.

28 March 1995
Electronics Letters Online No: 19950584

H. Yuen and L. Hanzo (*Department of Electronics and Computer Science, University of Southampton, Southampton SO17 1BJ, United Kingdom*)

References

1 ARNBAK, J.C., BONS, J.H., and VIEVEEN, J.W.: 'Graphical correspondence in electronic-mail networks using personal computers', *IEEE J. Sel. Areas Commun.*, 1989, **SAC-7**, pp. 257–267

2 LIU, K., and PRASAD, R.: 'Performance analysis of differential chain coding', *Eur. Trans. Telecomm. Relat. Technol.*, 1992, **3**, pp. 323–330

3 JOHANNESSEN, A.B., PRASAD, R., WEYLAND, N.B.J., and BONS, J.H.: 'Coding efficiency of multiring differential chain coding', *IEE Proc. I*, 1992, **139**, pp. 224–232

4 NEUHOFF, D.L., and CASTOR, K.G.: 'A rate and distortion analysis of chain codes for line drawings', *IEEE Trans.*, 1985, **IT-31**, pp. 53–68

Automatic pedestrian counting using image processing techniques

X. Zhang and G. Sexton

Indexing terms: Image processing, Computer vision

A new image processing algorithm used for pedestrian counting is introduced. The algorithm was ported to a TMS320C50 based platform and performs the pedestrian counting task in real time. The system has been tested at St Lazare Railway Station in Paris with better than 80% accuracy in the counting results.

Introduction: Recently the demand for real time pedestrian counting has increased for locations, such as railway stations, airports, large stores for building management and pedestrian traffic monitoring [1, 2]. In the past, many techniques have been developed for counting, such as using optical beams, microwaves and turnstiles, but they can only be used in constrained areas, such as narrow entrances. For unconstrained areas, at present, pedestrian flow information can only be obtained manually at a high cost and is not available in real time. The Esprit project PEDMON (6089) addressed the development of a novel image processing system for the purposes of automatically counting pedestrians.

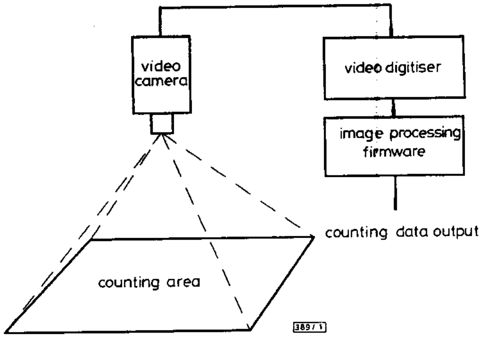

Fig. 1 *Image processing sensor system for pedestrian counting*